ORGANISATION EUROPEENNE POUR LA RECHERCHE NUCLEAIRE
EUROPEAN ORGANIZATION FOR NUCLEAR RESEARCH

Laboratoire Européen pour la Physique des Particules
European Laboratory for Particle Physics

Technical Inspection and Safety Division

Technical Note
CERN-TIS-2003-011-RP-TN

A comparison between Hg and Ta as material for a high power target from a radiation protection point of view

M. Magistris[1] and M. Silari

[1] Technical student in AB Division

Abstract

The future Superconducting Proton Linac (SPL) will provide a 2.2 GeV, 4 MW proton beam to feed facilities like, for example, a Neutrino Factory or a Neutrino SuperBeam. The induced radioactivity in the target station of such facilities is an important aspect that has to be taken into account at an early design stage. In particular, the choice of the target has consequences on the induced radioactivity and dose rates in the target station and its surroundings. In the present work, the radiological aspects of a stationary target made up of Ta pellets as proposed by Peter Sievers are compared to those of a free-surface jet of mercury.

CERN, 1211 Geneva 23, Switzerland
29 July 2003

1. Introduction

The future Superconducting Proton Linac (SPL) will provide a 4 MW, 2.2 GeV proton beam, which could be used by different facilities like, for example, a Neutrino Factory or a Neutrino SuperBeam. In such facilities, the proton beam impinges on a suitable target to produce pions, which are focused by a magnetic horn into a decay channel, where they decay into muons [Has00]. Theses muons are either accelerated to higher energies (in a Neutrino Factory) or generate directly a neutrino beam in their decay (a so-called Neutrino SuperBeam).

One of the main challenges is for such a system to sustain a 4 MW proton beam with a high pulse repetition rate (50 Hz) in a relatively small volume target (about 200 cm^3); indeed, the efficiency of the pion collection system decreases considerably with increasing target volume. To obtain high pion-production per unit target length, the best candidates as target materials are those with a high atomic number [Gil02].

At the present stage, the two most promising target candidates are a free-surface jet of mercury [Ama01] and the tantalum spheres proposed by Peter Sievers [Sie01]. After a brief description of the two designs, this note discusses the consequences of the target choice on the induced radioactivity in the target station.

2. The Hg and Ta targets

The essential feature of the mercury target is that the target is presented to the proton beam as a continuous free-surface liquid jet with ~15 mm diameter and 30 cm length. The jet is rapidly reformed after each beam pulse and allows the heat to be carried away efficiently from the production region without the need for nearby beam windows. After being irradiated, mercury will circulate for some ten seconds through a cooling system before being pumped again against the beam. The exact amount of mercury recirculating in the system is not yet known. If we assume that the mercury jet will be renewed with a frequency of 50 Hz, and that after being irradiated it will circulate for 10 s in the cooling system, we obtain that the mass of mercury is:

$$(0.75^2 \cdot \pi \cdot 30 \text{ cm}^3) \cdot (50 \text{ Hz}) \cdot (10 \text{ s}) \cdot (13.546 \text{ g cm}^{-3}) \approx 360 \text{ kg}, \qquad (1)$$

where 13.546 g cm^{-3} is the density of mercury at 20 °C.

Taking into account the time needed to pump the mercury from and to the cooling system, in this note it has been assumed that a total of ~500 kg of mercury will recirculate during operation. This is most likely a lower estimate; the real amount may be in the range from 5 to 10 tons.

Mercury has many advantages: it provides a source with good brightness because of its high density and the pion production yield is high, because of the cross section. Moreover, mercury is liquid at ambient temperature (there is no liquid-to-solid phase transition issue) and it does not present the problems of radiolysis like other liquid materials. On the other hand, from the point of view of radiation protection, the use of a mercury target raises high concern, since it has both the disadvantages of generating liquid radioactive waste and a lot of spallation products due to its high atomic mass. The latter characteristic implies that proton bombardment produces a very large number of radioactive nuclides. In addition, the storage of liquid radioactive waste may be subjected to severe restrictions from a regulatory point of view. Mercury may thus require to be solidified on site with a special treatment when becoming waste: it could be transformed into mercury sulphide (HgS), which is almost insoluble and has a high melting point (641 K). Although the process of solidification of non-radioactive mercury, in spite of its chemical toxicity,

is technically feasible, the high induced radioactivity will impose strict constraints on the handling of the large amounts required.

An alternative to the mercury target is the stationary target proposed by Peter Sievers [Sie01]. For such target, it is proposed to use solid spheres of tantalum with diameter in the millimetre range. These spheres are confined inside a titanium container and cooled by water or He. One of the major advantages of this solid target is that the amount of irradiated material is considerably reduced (~3 kg of Ta instead of ~500 kg or more of Hg) and can be stored after the shutdown of the facility without the need of processing. However, the open issue of the lifetime of such a structure and its fatigue limit must still be assessed.

3. FLUKA simulations

A first estimate of the induced radioactivity in the Hg target and the surrounding structures, i.e. the magnetic horn, the target cave, the decay pipe, the tunnel wall housing it and the surrounding rock were recently performed [Ago03]. In this note a comparison is made of the residual radioactivity expected in the facility when Ta is used instead of Hg as a target. Since this is just a preliminary study, in the calculations the Ta target was approximated with a solid cylinder rather than representing it in its real geometry. The results are normalized per proton incident on target and not per pion produced.

An estimate of the material activation and of the fluence of secondary protons and neutrons expected in the target station was performed by the Monte Carlo cascade code FLUKA [Fas00a, Fass00b]. The target station, which is considered to be built underground, consists of a target (either Hg or Ta), a magnetic horn and a decay tunnel. In the geometry simulated it is shielded by 2.6 m thick wall of concrete and is embedded in the rock (figure 1) [Ago03].
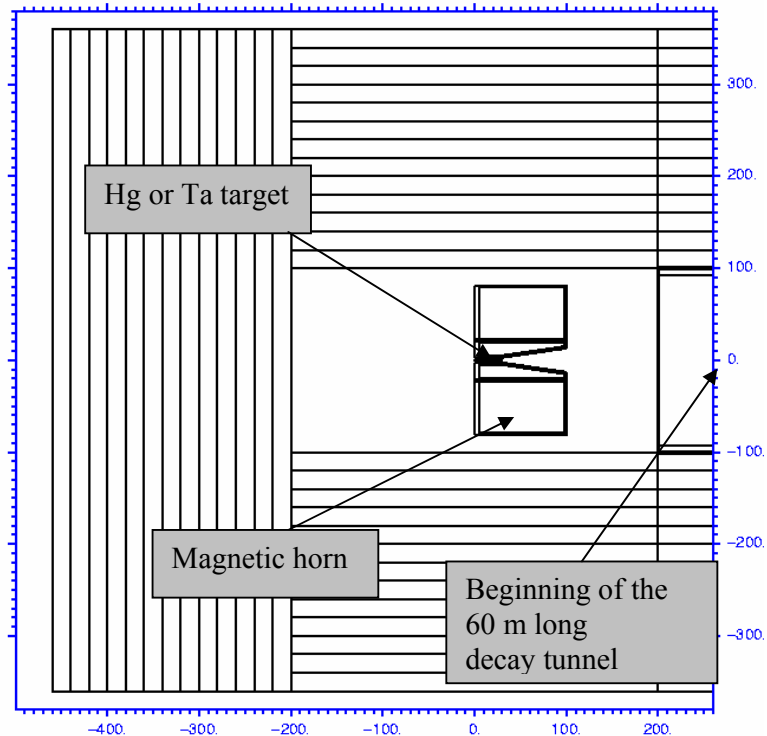
Figure 1. Side cross-sectional view of the target station with the concrete wall divided into 13 layers for scoring the residual nuclei distribution. The scales are in cm.

The source of particles has been defined as a 4 MW, 2.2 GeV proton beam with a Gaussian profile ($\sigma = 0.3$ cm) and without momentum spread or divergence. A magnetic horn consisting of two concentric annular cylinders (powered by currents of 300 kA and 600 kA, respectively) surrounds the target for focusing the produced pions. Downstream of the horn system, primary and secondary particles will enter a decay tunnel, along which most of the pions will decay into muons. The tunnel (60 m long with a diameter of 2 m) consists of 2.6 m thick wall of concrete and is surrounded by a deep layer of molasse, the typical geological formation in the Geneva area. The inner surface of the decay tunnel consists of a 1.6 cm thick layer of steel.

The horn is made of ANTICORODAL 110 Alloy with a density of 2.7 g cm^{-3} and the following chemical composition (weight fractions): Al 96.1%, Si 1%, Mg 1% and traces of Fe, Cu, Mn, Cr, Ni, Zn and Ti. The inner surface of the tunnel was assumed to be made of steel P355NH, like the decay pipe of the CNGS facility [Vin02]. Its chemical composition is: Fe 96.8%, Mn 1.65%, Si 0.5%, Cr 0.3%, Ni 0.3%, C 0.2% with traces of P and S. The concrete wall has a density of 2.35 g cm^{-3} and the following composition: O 50%, Si 20%, Ca 19.5%, Al 3%, C 3%, Fe 1.4%, Na 1%, K 1%, H 0.6% and Mg 0.5%. The molasse was given a density of 2.4 g cm^{-3} and the following composition: O 49%, Si 20%, Ca 9.7%, Al 6.4%, C 5%, Fe 3.9%, Mg 3.2%, K 1%, Na 0.5% and Mn 0.1%.

A total of 10 independent simulations were run for each target, each simulation transporting 500,000 primary protons. All particles were transported with an energy threshold of 10 MeV except pions (energy threshold: 10 keV), protons (energy threshold: 1 MeV) and neutrons (down to thermal energies). The magnetic field in the horn was taken into account and some biasing techniques were employed to reduce the statistical uncertainty, in particular inside the concrete wall.

4. The induced radioactivity in the target material

The mercury target was defined as a 30 cm long cylinder (radius: 0.75 cm) with a volume of 53 cm^3 and a density of 13.546 g cm^{-3} (figure 2). A total amount of 0.0369 m^3 of liquid is supposed to circulate in the system; the total activity induced in the cylinder was thus divided by 500,000 g to obtain the specific activity, assuming that mercury will be uniformly irradiated.

The stationary target filled with small tantalum spheres ($\rho = 16.6$ g cm^{-3}) was approximated as an homogenous cylinder made of tantalum, with an effective density $\rho_{eff} = 10$ g cm^{-3} [Sie01]; the volume (286 cm^3), the external shape and the weight (2.861 kg) of the target were respected. The tantalum target was thus defined as a 18 cm long cylinder (radius: 2.25 cm) surrounded by a 0.25 cm thick layer of titanium, representing the container enclosing the pellets.
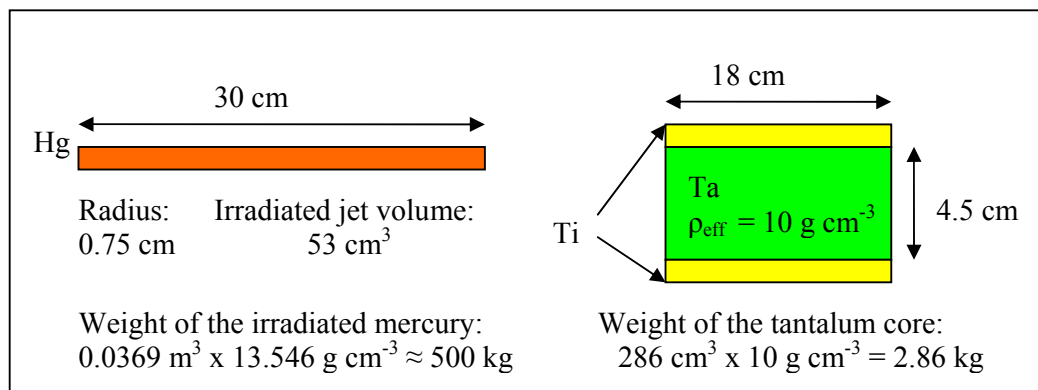
Figure 2. Layout of the mercury and the tantalum targets.

After the shutdown of the facility, the induced radioactivity expected in the target (figure 3) is similar for the two materials, although the tantalum target has a lower effective density and mercury has a higher atomic number. Although cross-sections play an important role in material activation, the activation also depends on the fact that the amount of mercury that is directly exposed to the proton beam (i.e., the mercury contained in the jet) is small when compared to the amount of tantalum contained in the stationary target. The ratio of the two is given by:

$$\frac{W_{Hg}}{W_{Ta}} = \frac{0.718\,kg}{2.861\,kg} \cong 0.25, \tag{2}$$

where W_{Hg} is the mass of mercury directly exposed to the proton beam and W_{Ta} is the mass of tantalum contained in the stationary target.
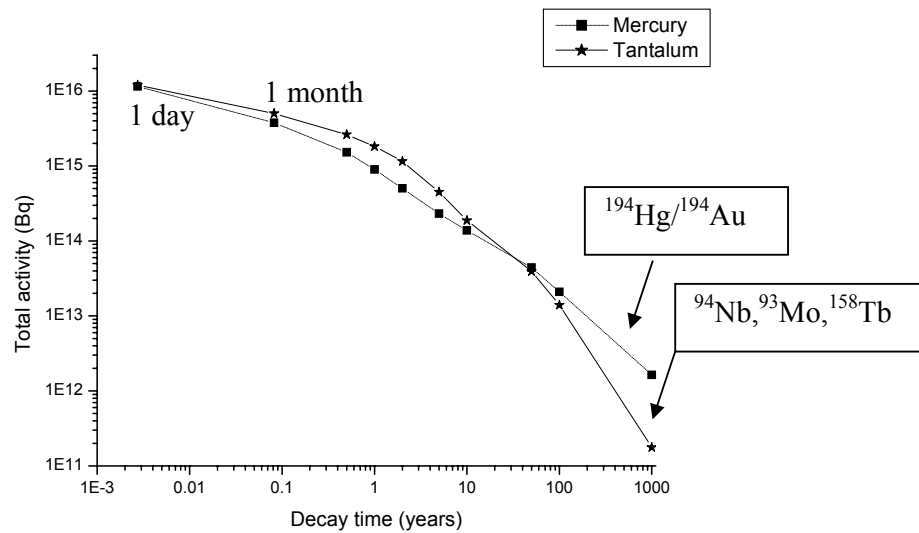
Figure 3. Induced radioactivity (Bq) in mercury and in tantalum after 10 years of operation, as a function of decay time. ^{194}Au is in secular equilibrium with ^{194}Hg ($T_{1/2} = 520$ y).

It is no surprise that the number of inelastic interactions (stars) scored in mercury (~1.22 stars per primary proton) is close to the number of stars scored in tantalum (~1.31 stars per primary proton), because both targets have been conceived for obtaining the same pion production efficiency (number of pions produced per primary proton), which is somehow related to the number of nuclear interactions of primary protons with the target nuclei.

For the same amount of induced radioactivity, different radioactive nuclides with different activities are expected in the two targets after the shutdown of the facility. In particular, no isotope heavier than tungsten was scored in the stationary target, whilst heavy gamma-emitters like ^{194}Au were found in mercury. Here "scored" means contributing to the induced activity for more than approximately 1% of the total. One hundred years after the shutdown of the facility, ^{194}Au is responsible for more then 95% of the gamma-emissions in the Hg-target. On a very long time scale, the most important gamma emitters in tantalum are ^{94}Nb, ^{93}Mo and ^{158}Tb. However, a large contribution to gamma emissions will also come from the annihilation of positrons emitted by ^{163}Ho, ^{91}Nb and ^{157}Tb. Tables 1-3 provide a list of the most

important radioactive nuclides scored in each target after 10 years of operation and 1, 10 and 100 years of decay, respectively.

Table 1. The most important radioactive nuclides scored in tantalum and mercury after 10 years of operation and 1 year of decay. All results have a statistical uncertainty lower than 1.5%. The nuclides marked with γ are responsible for ~90% of the total energy emitted through gamma radiation.

Residual nuclei after 10 year operation and 1 year decay		Activity (Bq)	
Isotope	Half-life	Tantalum	Mercury
^{3}H	12.3 y	$4.89 \cdot 10^{13}$	$\mathbf{5.55 \cdot 10^{13}}$
^{54}Mn (γ)	312 d	$2.52 \cdot 10^{12}$	$\mathbf{3.15 \cdot 10^{12}}$
^{60}Co (γ)	5.27 y	$1.85 \cdot 10^{12}$	$\mathbf{3.56 \cdot 10^{12}}$
^{88}Y (γ)	106 d	$2.11 \cdot 10^{12}$	$\mathbf{4.81 \cdot 10^{12}}$
^{145}Pm	17.7 y	$\mathbf{1.18 \cdot 10^{14}}$	$5.51 \cdot 10^{13}$
^{145}Sm	340 d	$\mathbf{1.34 \cdot 10^{14}}$	$5.63 \cdot 10^{13}$
^{149}Eu	93.1 d	$\mathbf{4.00 \cdot 10^{13}}$	$1.97 \cdot 10^{13}$
^{148}Gd	74 y	$\mathbf{1.98 \cdot 10^{13}}$	$1.03 \cdot 10^{13}$
^{151}Gd	124 d	$\mathbf{4.37 \cdot 10^{13}}$	$2.25 \cdot 10^{13}$
^{153}Gd	241 d	$\mathbf{7.43 \cdot 10^{13}}$	$3.71 \cdot 10^{13}$
^{172}Lu (γ)	6.7 d	$\mathbf{1.79 \cdot 10^{14}}$	$6.77 \cdot 10^{13}$
^{173}Lu (γ)	1.37 y	$\mathbf{2.17 \cdot 10^{14}}$	$7.72 \cdot 10^{13}$
^{172}Hf (γ)	1.87 y	$\mathbf{1.77 \cdot 10^{14}}$	$6.71 \cdot 10^{13}$
^{179}Ta	1.79 y	$\mathbf{6.49 \cdot 10^{14}}$	$1.42 \cdot 10^{14}$
^{181}W	121 d	$1.36 \cdot 10^{12}$	$\mathbf{2.60 \cdot 10^{13}}$
^{185}Os (γ)	93.6 d	-	$\mathbf{2.81 \cdot 10^{13}}$
^{193}Pt	50 y	-	$\mathbf{3.36 \cdot 10^{13}}$
^{194}Hg /^{194}Au (γ)	520 y	-	$\mathbf{2.83 \cdot 10^{12}}$
^{195}Au	312 d	-	$\mathbf{1.11 \cdot 10^{14}}$
Total radioactivity (Bq)		$1.8 \cdot 10^{15}$	$8.9 \cdot 10^{14}$

Table 2. The most important radioactive nuclides scored in tantalum and mercury after 10 years of operation and 10 years of decay. All results have a statistical uncertainty lower than 1.5%. The nuclides marked with γ are responsible for ~90% of the total energy emitted through gamma radiation.

Residual nuclei after 10 year operation and 10 year decay		Activity (Bq)	
Isotope	Half-life	Tantalum	Mercury
^{3}H	12.3 y	$2.94 \cdot 10^{13}$	$\mathbf{3.35 \cdot 10^{13}}$
^{60}Co (γ)	5.27 y	$5.72 \cdot 10^{11}$	$\mathbf{1.09 \cdot 10^{12}}$
^{133}Ba (γ)	10.5 y	$\mathbf{3.89 \cdot 10^{12}}$	$5.38 \cdot 10^{11}$
^{145}Pm	17.7 y	$\mathbf{9.09 \cdot 10^{13}}$	$4.23 \cdot 10^{13}$
^{148}Gd	74 y	$\mathbf{1.82 \cdot 10^{13}}$	$9.50 \cdot 10^{12}$
^{172}Lu (γ)	6.7 d	$\mathbf{6.35 \cdot 10^{12}}$	$2.43 \cdot 10^{12}$
^{172}Hf (γ)	1.87 y	$\mathbf{6.29 \cdot 10^{12}}$	$2.41 \cdot 10^{12}$
^{179}Ta	1.79 y	$\mathbf{1.98 \cdot 10^{13}}$	$4.34 \cdot 10^{12}$
^{193}Pt	50 y	-	$\mathbf{2.97 \cdot 10^{13}}$
^{194}Hg /^{194}Au (γ)	520 y	-	$\mathbf{2.80 \cdot 10^{12}}$
Total radioactivity (Bq)		$1.8 \cdot 10^{14}$	$1.4 \cdot 10^{14}$

Table 3. The most important radioactive nuclides scored in tantalum and mercury after 10 years of operation and 100 years of decay. All results have a statistical uncertainty lower than 1.5%. The nuclides marked with γ are responsible for ~90% of the total energy emitted through gamma radiation.

Residual nuclei after 10 year operation and 100 year decay		Activity (Bq)	
Isotope	Half-life	Tantalum	Mercury
^{42}K (γ)	12.4 h	6.98·10^9	**1.66·10^{10}**
^{44}Sc (γ)	3.9 h	3.11·10^9	**4.57·10^9**
^{133}Ba (γ)	10.5 y	**1.03·10^{10}**	1.42·10^9
^{145}Pm	17.7 y	**2.68·10^{12}**	1.24·10^{12}
^{148}Gd	74.6 y	**7.92·10^{12}**	4.11·10^{12}
^{150}Eu (γ)	38.8 y	**3.81·10^9**	2.95·10^9
^{157}Tb	99 y	**2.86·10^{12}**	1.33·10^{12}
^{158}Tb (γ)	180 y	**2.02·10^9**	8.94·10^8
^{193}Pt	50 y	-	**8.55·10^{12}**
^{194}Hg /^{194}Au (γ)	520 y	-	**2.48·10^{12}**
Total radioactivity (Bq)		1.4·10^{13}	2.1·10^{13}

Similarities can be expected in terms of radiation damage, generation of prompt radiation and residual radioactivity between the SPL target and the target designed for the European Spallation Source (ESS). Although the ESS design is for a neutron-producing target, the total proton beam power is comparable with the present neutrino-production facility. Indeed, the values of total activity in tables 1-3 are of the same order as those estimated for the ESS mercury target. For a 15-ton mercury target and one *full* year of operation at 5 MW, the total radioactivity after 1, 10 and 100 years of decay is 1.3·10^{15} Bq, 4.9·10^{13} Bq and 1.4·10^{11} Bq, respectively (table 4.2.3 of Ref. [ESS96]). Discrepancies are mainly due to different beam characteristics, irradiation times and irradiated target volume (which is larger in the ESS design).

5. The induced radioactivity in the target station

The production and the distribution of secondary particles in the target station depend slightly on the target. Figure 4 shows the proton fluence rate (cm^{-2} s^{-1}) expected in the target station during operation with a tantalum and a mercury target. The scale of colours is the same in both plots. Values vary from 10^9 cm^{-2} s^{-1} (white) to 10^{15} cm^{-2} s^{-1} (black).

The proton fluence rate downstream of the target appears better focused in the case of tantalum, because the mercury target is thicker and with a higher atomic number and therefore more protons are scattered from their original trajectory or are slowed down. The same is valid for the secondary protons generated in the intranuclear cascade. For the same reason, protons entering the decay tunnel are expected to have higher energy in the case of tantalum. Figure 5 shows the differential current density of protons entering the tunnel; in this context, current density is defined as the number of particles crossing a boundary surface per unitary area and per primary particle.

Because the transverse dimension of the mercury jet is smaller than that of the stationary target, the self-absorption is also smaller. Thus fewer (40%-60%) protons will strike the magnetic horn which surrounds the target in the case of tantalum, as shown in figure 6.
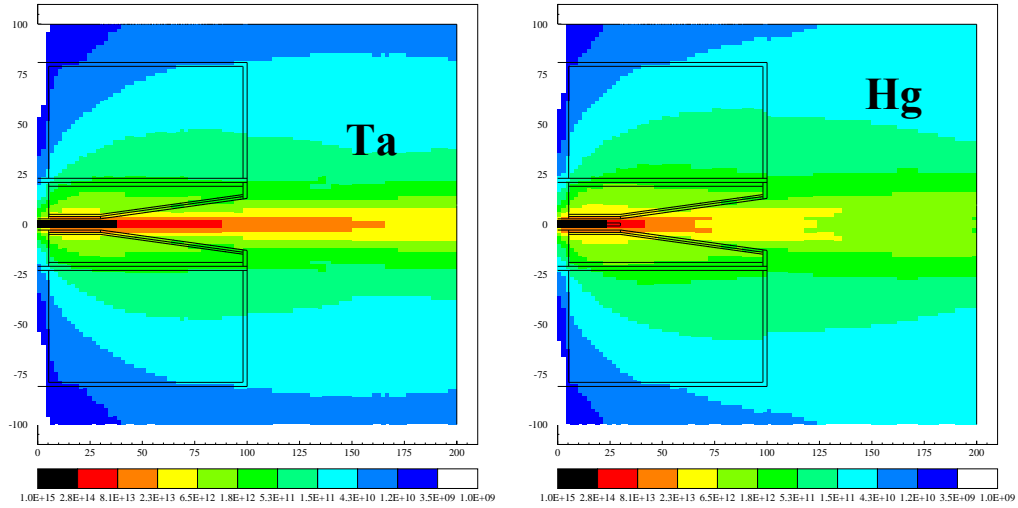
Figure 4. Proton fluence rate (cm^{-2} s^{-1}) in the target station.
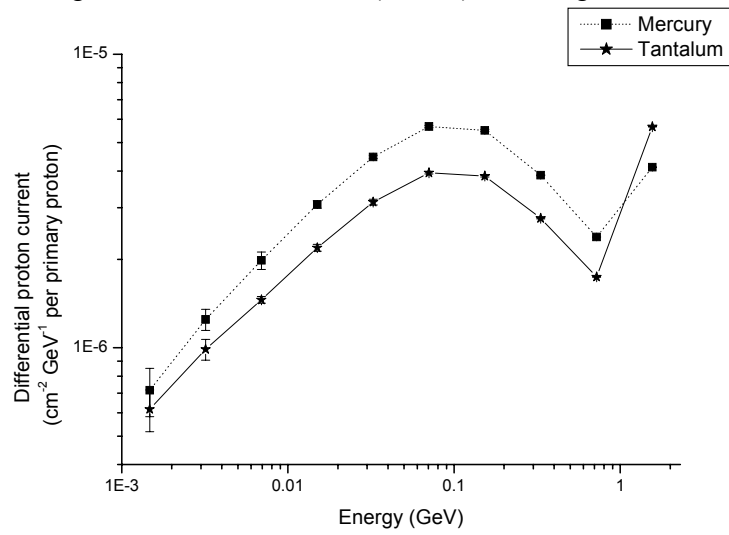
Figure 5. Differential current density (cm^{-2} GeV^{-1} per primary proton) of protons entering the decay tunnel.
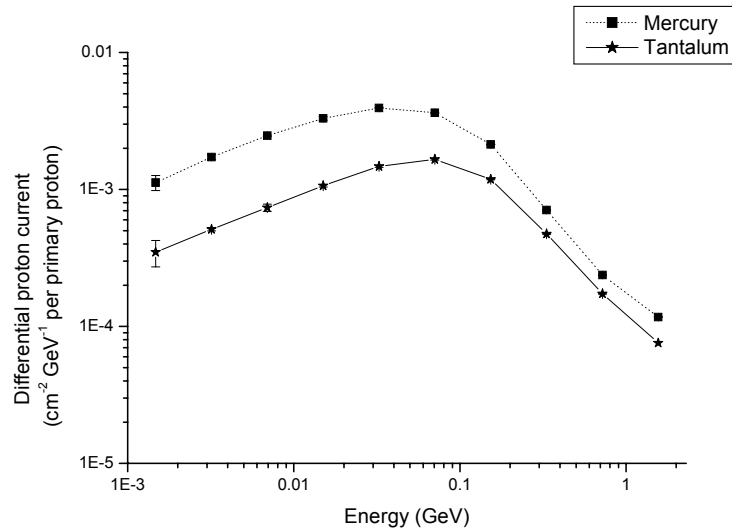
Figure 6. Differential current density (cm^{-2} GeV^{-1} per primary proton) of protons striking the magnetic horn.

8

The target material also affects the distribution of secondary neutrons, which give a great contribution to the material activation in the target station. The neutron fluence rate (cm^{-2} s^{-1}) expected in the target station during operation is shown in figure 7; it appears slightly higher in the case of mercury because of its higher atomic number. Values vary from $2.5 \cdot 10^{12}$ cm^{-2} s^{-1} (white) to $3.0 \cdot 10^{15}$ cm^{-2} s^{-1} (black).
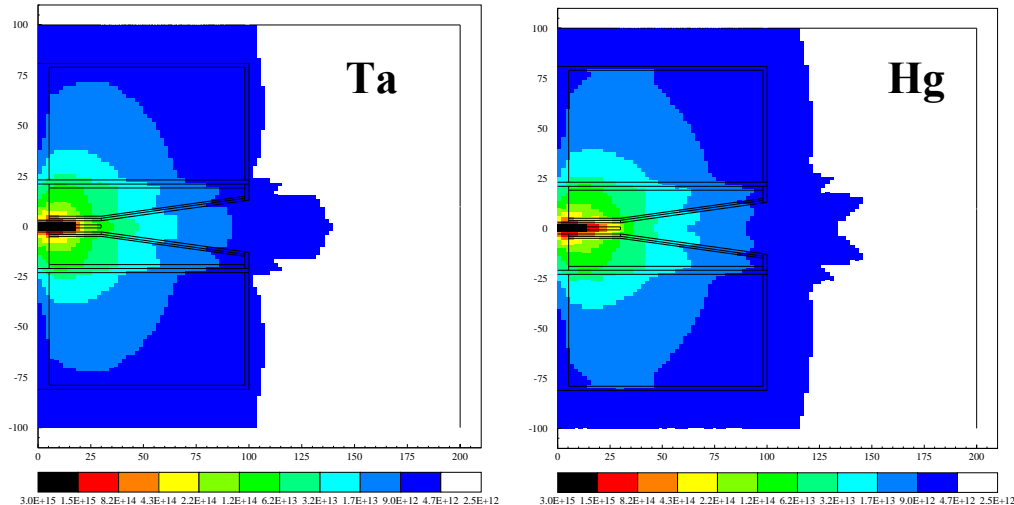
Figure 7. Neutron fluence rate (cm^{-2} s^{-1}) in the target station.

Figure 8 shows that the differential current density of neutrons entering the magnetic horn has the same shape for both targets, but slightly higher values in the case of mercury, especially for neutrons from 10 MeV to 1 GeV. This is due to the fact that on the one hand mercury has a higher mass number (and therefore more neutrons are produced), and on the other hand the mercury jet is thinner in the transverse dimension (and therefore less neutrons are self-absorbed in the target).

The induced radioactivity in the magnetic horn is mainly due to the neutrons produced in the target: secondary protons crossing the inner surface of the horn mostly activate its inner part. With respect to a mercury target, with a stationary Ta target both the number of 10-100 MeV neutrons (figure 8) and the activity of the outer part of the horn (figure 9) are reduced by ~20%. The activity in the inner part of the horn is reduced by ~40% (figure 9) also because of the reduced number of protons escaping from the lateral surface of the tantalum target (figure 4).

The differential current density (cm^{-2} GeV^{-1} per primary proton) of neutrons entering the decay tunnel is shown in figure 10. Although the neutron current density does not depend on the choice of the target material for low-energy neutrons, the current of neutrons in the 10-100 MeV range is reduced by ~30% in the case of a tantalum target. However, the higher number of high-energy protons entering the tunnel in the case of a Ta target increases the induced radioactivity in the steel pipe by ~20% (figure 11).

6. Dose rates

An estimation of the dose rate expected during maintenance operation and after the shutdown of the facility was obtained with the use of the software package MicroShield [Mic96]. For a given source of radioactivity and a defined geometry, MicroShield calculates numerically the dose rates expected at a given point from the source, only taking into account photons from gamma-emitters (in particular, gammas produced by annihilation of positrons are not considered).

9
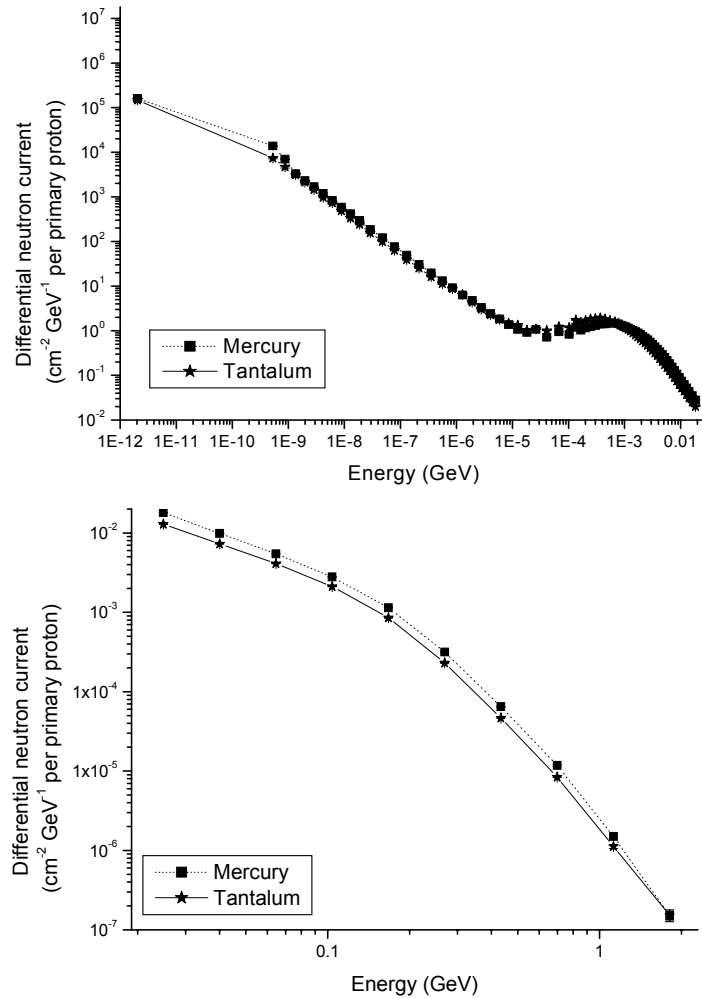
Figure 8. Differential current density (cm^{-2} GeV^{-1} per primary proton) of neutrons striking the magnetic horn. Top: thermal to 10 MeV neutrons, bottom: 10 MeV-2 GeV neutrons. The choice of a tantalum target reduces by ~20% the number of neutrons in the 10-100 MeV range crossing the magnetic horn surface.
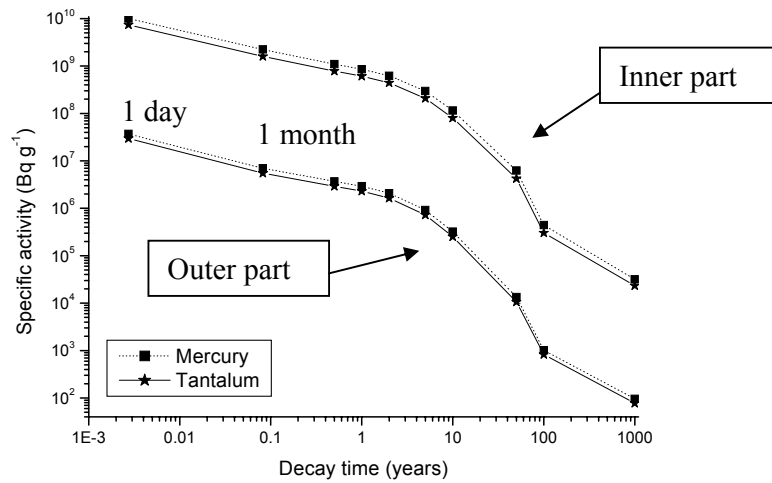
Figure 9. Induced specific radioactivity (Bq g^{-1}) in the magnetic horn after 6 weeks of irradiation. The choice of a tantalum target reduces by ~40% the induced radioactivity in the inner part of the horn.
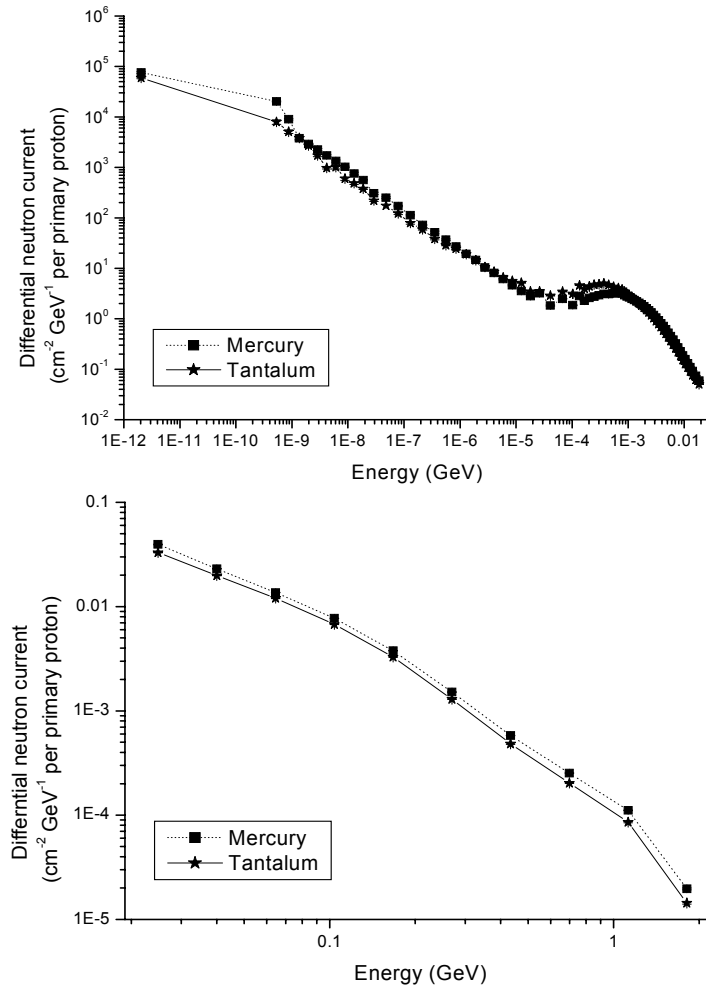
Figure 10. Differential current density (cm^{-2} GeV^{-1} per primary proton) of neutrons entering the decay tunnel. Top: thermal to 10 MeV neutrons, bottom: 10 MeV-2 GeV neutrons. The choice of a tantalum target reduces by ~30% the number of neutrons in the 10-100 MeV range.
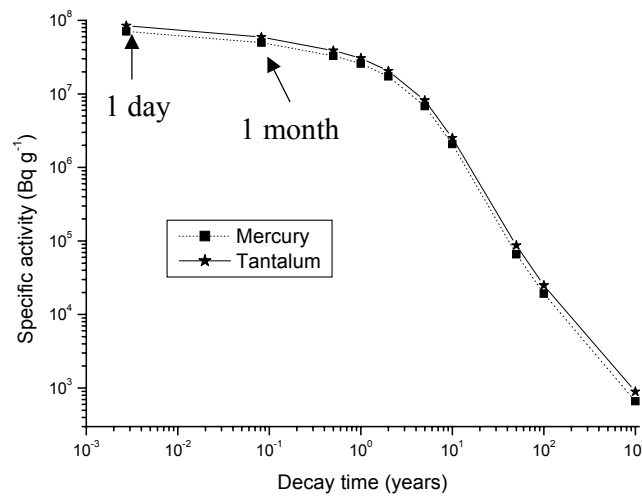
Figure 11. Induced radioactivity in the steel pipe of the decay tunnel after 10 years of operation. The choice of a mercury target reduces by ~20% the induced radioactivity in the pipe.

The ambient dose equivalent rate H*(10) [Don03] expected at 1 m from the Ta target after 10 years of operation and 1 year of decay, if the target is never replaced during the 10 years of operation, is 23.6 Sv h^{-1}. If we assume that after the shutdown of the facility all mercury is stored in a spherical tank (radius: 20.6 cm), after 10 years of operation and 1 year of decay the H*(10) expected at 1 m from the tank surface is 1.1 Sv h^{-1}. Such a different value of dose rate for almost the same induced radioactivity is mainly due to the phenomenon of self-absorption in the target, which is much more effective in mercury (~500 kg of liquid) then in the small stationary target (~3 kg of tantalum). However, due to its relatively small size, a tantalum target can be easily shielded and in the end, for the same volume (waste + shielding), the dose rates expected at some distance from a Ta and an Hg target are similar.

The induced radioactivity in the horn depends to some extent on the target, as shown in figure 9. The H*(10) expected at 1 m from the horn after 6 weeks of irradiation and 1 day of decay is 8 Sv h^{-1} in the case of tantalum and 9.9 Sv h^{-1} in the case of mercury. These values only take into account the gammas emitted by the horn and not by other components like, for example, the wall of the target station or the cooling system.

The real life-time of the tantalum target is not yet known. A shorter life-time of the target would increase the amount of irradiated tantalum and decrease its mean specific activity. The total radioactivity induced in tantalum depends only on the proton beam intensity (primary particles per second) and on the irradiation cycle and is independent of the number of targets irradiated. However, a larger amount of tantalum would reduce the dose rate expected at some distance from the irradiated targets because of the phenomenon of self-absorption. Considering shorter life-times of the Ta target would thus reduce the dose rate expected in the target station during the horn replacement (table 4). Calculations were done under the assumption that the target would be replaced together with each horn (i.e., every six weeks) or only twice or once per year. Finally, a target life-time of 10 years was also considered.

Table 4. Ambient dose equivalent rates H*(10) expected during horn replacement and after the shutdown of the facility for different life-times of the Ta target.

Life-time of the tantalum target	Dose rate (Sv h^{-1}) expected at 1 m from the horn, one day cooling time				Dose rate at 1 m from irradiated Ta, one year after the final shutdown	
	Horn (*)	Ta target	Ti container	Total	Waste volume (Ta)	Dose rate, Sv h^{-1}
6 weeks	8.0	30.7	0.9	39.6	11,444 cm^3	7.2
2 x 6 weeks	8.0	38.4	1.2	47.6	5,772 cm^3	9.1
1 year of operation (4 x 6 weeks)	8.0	42.2	1.5	51.7	2,861 cm^3	15.3
10 years of operation	8.0	46.3	1.6	55.9	286.1 cm^3	23.6

(*) The dose rate due to the horn does not depend on the target life-time since the horn will anyway be replaced every 6 weeks, because of mechanical stress.

7. A comparison between 2.2 and 4 GeV beam energies

The induced radioactivity in the facility mainly depends on the beam power and on the primary-proton kinetic energy. Whilst one can expect that globally the material activation increases linearly with increasing beam power, its correlation with particle energy is somehow more complicated, as it depends on multiplicity, type and

energy spectrum of the secondary particles produced. In order to estimate the total activity induced in the target station by protons with higher kinetic energy, two sets of simulations were run for beam energy of 4 GeV (value arbitrarily chosen) and the results are shown in table 5. For the same beam power (4 MW), the induced radioactivity in the target station changes only slightly with increasing proton energy (table 6).

Table 5. Total activity in the target, the magnetic horn, a 2.6 m thick concrete wall and the surrounding rock induced by 2.2 GeV and 4 GeV proton beams, sent onto an Hg and a Ta target. Values refer to 10 years of operation (target, concrete and rock) or 6 weeks of continuous irradiation (magnetic horn), followed by different waiting times.

Hg	Total activity (Bq)							
	1 month decay		1 year decay		10 year decay		100 year decay	
	2.2 GeV	4 GeV	2.2 GeV	4 GeV	2.2 GeV	4 GeV	2.2 GeV	4 GeV
Target	3.7E15	3.4E15	8.9E14	1.0E15	1.4E14	3.0E14	2.1E13	1.9E13
Horn	2.4E13	2.3E13	9.6E12	8.9E12	1.2E12	1.1E12	4.2E9	4.1E9
Concrete	2.2E15	2.2E15	7.3E14	7.3E14	2.5E14	2.5E14	4.8E12	4.7E12
Rock	5.6E12	5.4E12	2.1E12	2.2E12	5.2E11	5.1E11	1.0E10	8.7E9

Ta	1 month decay		1 year decay		10 year decay		100 year decay	
	2.2 GeV	4 GeV	2.2 GeV	4 GeV	2.2 GeV	4 GeV	2.2 GeV	4 GeV
Target	5.0E15	3.8E15	1.8E15	1.5E15	1.9E14	2.5E14	1.4E13	1.0E13
Horn	1.8E13	1.5E13	7.2E12	6.1E12	8.7E11	7.8E11	3.2E9	3.0E9
Concrete	1.6E15	1.6E15	1.1E15	1.1E15	2.0E14	2.1E14	1.1E12	1.1E12
Rock	2.2E12	2.0E12	1.5E12	1.4E12	2.1E11	2.0E11	1.5E9	9.5E8

Table 6. Ratio of total activities, Activity (4 GeV)/Activity (2.2 GeV), in the components of the target station, for different decay times.

	Mercury target				Tantalum target			
	1 month	1 year	10 years	100 years	1 month	1 year	10 years	100 years
Target	0.92	1.12	2.14	0.90	0.76	0.83	1.31	0.71
Horn	0.96	0.93	0.92	0.92	0.83	0.85	0.90	0.94
Concrete	1.00	1.00	1.00	0.98	1.00	1.00	1.05	1.00
Rock	0.96	1.05	0.94	0.87	0.91	0.93	0.95	0.63

Material activation in the magnetic horn, in the concrete wall and in the surrounding rock is more important in the case of an Hg target than of a Ta target. The induced radioactivity in the target is lower for Hg on short time scales (less than 10 years) and for Ta on long time scales (more than 10 years). In the case of a 4 GeV proton beam, the production of tritium is relatively high in both the Hg and the Ta targets: tritium is the most abundant nuclide in the irradiated target material 10 years after the irradiation period. Table 7 shows the number of inelastic interactions, of secondary particles created and of high-energy fissions per second in the various components of the facility.

8. Conclusions

Although the total activity induced in the target depends only weakly on the material, different isotopes are produced in tantalum and in mercury, resulting in different decay times. In particular, on very long time scales (longer than a few hundred years) the residual ^{194}Hg/^{194}Au makes mercury ~10 times more radioactive than tantalum. The neutron fluence rate in the target station during operation is lower

in the case of tantalum and therefore the induced radioactivity in the magnetic horn is reduced by ~20%.

Table 7. Number of inelastic interactions (stars) and secondary particles created in the target station per second.

(Values are in s^{-1})	2.2 GeV proton beam		4 GeV proton beam	
	Hg	Ta	Hg	Ta
Stars	1.6E17	1.7E17	1.4E17	1.4E17
Secondaries created	9.0E17	1.0E18	7.8E17	8.5E17
High-energy fissions	1.2E15	5.3E14	8.8E14	4.4E14
Low-E neutron sec. (*)	2.8E19	4.9E19	2.4E19	4.1E19

(*) Secondaries created per second in low-energy neutron interactions.

On the one hand, fewer high-energy protons enter the decay tunnel in the case of a mercury target and therefore the induced radioactivity in the decay pipe appears reduced by 20%. Furthermore, the phenomenon of self-absorption reduces the dose rate expected at some distance from the mercury container with respect to a Ta target, after the shutdown of the facility.

On the other hand, the stationary target has the great advantage of being solid, and thus does not require to be solidified with a special treatment when becoming waste. If the target life-time is long enough to cover the whole period of operation, only ~3 kg of tantalum are activated (to be compared with ~500 kg or more of liquid Hg) and the waste storage appears easier. In this case, the tantalum target could in principle be retrieved from the magnetic horn and temporarily stored in a shielded place during horn substitution, so that the target contribution to the total dose rate (~40 Sv h^{-1}, table 4) would be strongly reduced. One can always envisage changing the Ta target together with the horn every 6 weeks of operation. In this case more waste would be produced, but with a lower activity per target. Moreover, designing target and horn as an integrated system would possibly simplify their substitution and storage.

Raising the proton beam energy from 2.2 GeV to 4 GeV, maintaining the same beam power, increases the production of ^{3}H, but does not change substantially the total amount of induced radioactivity in the target material and in the surrounding components.

Whatever will be the final choice of the target material, there are three important radiation protection issues which will play an important role in the design of the target station: 1) the doses which will be received by personnel during maintenance (it is obvious that remote handling will be mandatory), 2) accident scenarios and 3) production and treatment of radioactive waste. Safety issues such as containment of radioactive material must be given due consideration ad these are obviously more critical with a liquid metal target than with a solid target. Vapour emission from the target and afterheat will also have to be evaluated. A facility handling a 4 MW beam will need formal authorisation by the Swiss and/or French authorities to operate and will be subjected to strict control from the Host State authorities. Before such an authorisation can be granted, the Laboratory hosting the facility will have to prove that the facility can be operated safely, with no impact on the environment both during routine operation and in case of an incident or accident, and that the aspects related to treatment and storage of the radioactive waste are properly taken into account.

The ESS study considered the option of both a solid target (plate or rod) made of tungsten or tantalum and a liquid mercury target [ESS96]. All target concepts were

found practical for their planned proton beam power of 5 MW. The ESS eventually chose a liquid metal target because of uncertainties about the effects of radiation damage and transient thermal stresses in the solid target option. Mercury was selected because it had advantages over lead or lead/bismuth for a pulsed source. A complete comparative study between various target designs should consider the pion production yield, the expected lifetime of the target, as well as the amount and the form of the radioactive waste generated.

In the ESS study it is stated that it is possible – in principle – to purify the target material to reduce its medium term radioactivity to very low level. Such a process will nonetheless still leave behind an important quantity of liquid metal waste. At present in Switzerland liquid radioactive waste is not accepted for final storage in a repository.

Acknowledgements

References

[Ago03]   S. Agosteo, M. Magistris, Th. Otto and M. Silari, *Induced radioactivity in a 4 MW target and its surroundings*, CERN-TIS-2003-003-RP-CF (2003).

[Ama01]   J. Amand, *Simulation of target particles emission for Neutrino Factory using FLUKA*, CERN-NUFACT Note 070 (2001).

[Don03]   Y. Donjoux, *Logiciel MicroShield Utilisation des grandeurs dosimétriques appropriées*, CERN-TIS-2003-007-RP-TN (2003).

[ESS96]   The ESS Technical Study, Volume III, ESS-96-53-M (1996).

[Fas00a]   A. Fassò, A. Ferrari and P.R. Sala, *Electron-photon transport in FLUKA: status*, Proc. of the MonteCarlo 2000 Conference, Lisbon (2000).

[Fas00b]   A. Fassò, A. Ferrari, J. Ranft and P.R. Sala, *FLUKA: Status and prospective for hadronic applications*, Proc. of the MonteCarlo 2000 Conference, Lisbon (2000).

[Fer96]   A. Ferrari, P.R. Sala, J. Ranft and S. Roesler, *Cascade particles, nuclear evaporation and residual nuclei in high-energy hadron-nucleus interactions*, Z. Phys. C70, 413-426 (1996).

[Gil02]   S. Gilardoni, *A European Neutrino Factory complex*, proceedings of ICHEP 2002, pp. 930-932, Amsterdam (2002).

[Has00]   H. Haseroth, *CERN ideas and plans for a Neutrino Factory*, CERN-NUFACT Note 045 (2000).

[Mic96]   *MicroShield Version 5, User`s manual*, Grove Engineering (1996).

[Sie01]   P. Sievers, *A stationary target for the CERN-Neutrino-Factory*, CERN-NUFACT Note 065 (2001).

[Vin02]   H. Vincke and G.R. Stevenson, *Induced radioactivity and dose rates in the decay tunnel of the CNGS facility*, Technical Note TIS-RP/TN/2002-013 (2002).